

Sum-over-states calculation of the nuclear spin–spin coupling constants

P. Bouř and M. Buděšínský

Institute of Organic Chemistry and Biochemistry, Academy of Sciences of the Czech Republic, Flemingovo 2, 16610 Prague 6, Czech Republic

(Received 31 July 1998; accepted 3 November 1998)

Nuclear spin–spin coupling constants calculated using the sum-over-states (SOS) expansions were compared to experimental values and usual coupled-perturbed (CP) calculations. Rigid Kohn–Sham orbitals obtained from a hybrid density functional were used in the SOS model. Its accuracy for small molecules is comparable with the CP results, nevertheless calculated constants were uniformly underestimated. However, the SOS scheme is less limited by molecular size and can be applied for bigger systems than the CP method, as documented on the proton–proton coupling constants in α -pinene, β -pinene, and camphor molecules. © 1999 American Institute of Physics. [S0021-9606(99)30506-7]

I. INTRODUCTION

Nuclear magnetic resonance (NMR) spectra provide a sensitive probe of molecular structure and interactions. The sensitivity is given by a long-range nonlocalized nature of the magnetic forces susceptible to fine perturbations of electronic density. This complexity makes *ab initio* predictions of NMR parameters difficult and the spectra have been interpreted rather on an empirical basis. However, powerful theoretical procedures have been developed and built into commercial software packages recently.^{1,2} Reliable computations namely of the magnetic shielding tensors are presently available even for larger molecules.³

Unlike for the shielding, computations of nuclear spin–spin coupling were discouraged in the past, since even for small molecules complicated post-HF expansions had to be used for meaningful results.⁴ Generally, also a vibrational averaging of calculated coupling constants is recommended for benchmark calculations. In spite of these difficulties the need of an *ab initio* modeling of the coupling is apparent, since it appears to be less affected by the solvent and is thus more closely related to molecular conformation than the shielding. As may be expected, the post-HF coupled-perturbed (CP) calculations are strongly limited by molecular size,¹ although this constrain becomes less stringent when the methodology of the density-functional theory (DFT) is used.^{5,6}

Previously, we have shown that computer demands required for computations of particular molecular properties can be significantly reduced when the sum-over-states (SOS) perturbation expansions are used instead of the CP techniques. For polarizabilities,⁷ vibrational circular dichroism (VCD)^{8,9} and Raman optical activity (ROA) spectra¹⁰ the SOS results were comparable with CP calculations for bigger molecules. In this study, we explore performance of a simple SOS scheme applied for calculation of the spin coupling. As shown below, present implementation is not suitable for benchmark calculations. However, it can be used for a computationally inexpensive estimation of the coupling for molecules unachievable by classical techniques. Moreover, un-

like other semiempirical methods, the SOS/DFT methodology is open to future improvements up to the Schrödinger limit. Since none of the most frequent exchange–correlation functionals explicitly contains magnetic part, we also consider it important from theoretical point of view to test the quality of calculations of magnetic properties using the density functional theory.

II. THEORY

Magnetic phenomena are included consistently in the Dirac relativistic equation.¹¹ However, nonrelativistic limit (Pauli equation) is usually sufficient for interpretation of NMR experiments. For the coupling, those terms involve the Fermi-contact term (FC), paramagnetic (PSO), diamagnetic spin–orbit (DSO) and spin–dipolar (SD) coupling^{12,13}

$$H = H_{\text{FC}} + H_{\text{SD}} + H_{\text{PSO}} + H_{\text{DSO}}, \quad (1)$$

where

$$H_{\text{FC}} = \frac{2\mu_B g_e \mu_0}{3\hbar} \sum_{n,N} \gamma_N \delta(r_{nN}) s_n \cdot I_N, \quad (2)$$

$$H_{\text{SD}} = \frac{g_e \mu_0 \mu_B}{4\pi\hbar} \sum_{n,N} \gamma_N \frac{3s_n \cdot r_{nN} r_{nN} \cdot I_N - r_{nN}^2 s_n \cdot I_N}{r_{nN}^5}, \quad (3)$$

$$H_{\text{PSO}} = \frac{e\mu_0}{4\pi m_e} \sum_{n,N} \frac{\gamma_N I_N \cdot l_{nN}}{r_{nN}^3}, \quad (4)$$

$$H_{\text{DSO}} = \frac{e^2 \mu_0^2}{(4\pi)^2 2m_e} \times \sum_{n,N,M} \gamma_N \gamma_M \frac{I_N \cdot I_M r_{nN} \cdot r_{nM} - I_N \cdot r_{nM} r_{nN} \cdot I_M}{r_{nN}^3 r_{nM}^3}. \quad (5)$$

Symbol μ_B (in $\text{m}^2 \text{C s}^{-1}$ for SI units used in this work) denotes the Bohr magneton; μ_0 [m kg C^{-2}] is the vacuum permeability; $g_e = 2.0023$; \hbar [J] the Planck constant; γ_N [C s^{-1}] and I_N [J s] the gyromagnetic ratio and spin of nucleus N , $\gamma_N = g_N \mu_N / \hbar$, where μ_N [$\text{m}^2 \text{C s}^{-1}$] is the nuclear magne-

ton; s_n [J s⁻¹], e [C], and m_e [kg] are the electronic spin, charge and mass, respectively; $l_{nN} = r_{nN} \times p_n$ [J.s], $r_{nN} = r_n - R_N$; r_n and p_n is electronic position and momentum, R_N is nuclear position.

The nuclear coupling tensor $J_{N\alpha M\beta}$ is defined as a second derivative of energy with respect to nuclear spins

$$J_{N\alpha M\beta} = \left[\frac{\hbar^2 \partial^2 E}{\partial I_{N\alpha} \partial I_{M\beta}} \right]_{\mu_N=0, \mu_M=0} \quad (6)$$

An alternative definition of the constant based on derivatives with respect to magnetic momenta as well as reduced coupling constants independent of isotopic species were also introduced.^{5,6} In experimental practice the tensor is usually expressed in Hz: $J_{N\alpha M\beta} [\text{Hz}] = (2\pi\hbar)^{-1} J_{N\alpha M\beta} [\text{J}]$. For isotropic samples a spatially averaged constant can be defined as

$$J_{NM} = \frac{1}{3} \sum_{\alpha=1}^3 J_{N\alpha M\alpha} \quad (7)$$

Introducing molecular ground state $|g\rangle$, expression (6) leads to

$$\begin{aligned} J_{N\alpha M\beta} &= 2\hbar^2 \left\langle \frac{\partial g}{\partial I_{M\beta}} \left| \frac{\partial H}{\partial I_{N\alpha}} \right| g \right\rangle + \hbar^2 \left\langle g \left| \frac{\partial^2 H}{\partial I_{M\beta} \partial I_{N\alpha}} \right| g \right\rangle \\ &= J_{N\alpha M\beta}^P + J_{N\alpha M\beta}^D \end{aligned} \quad (8)$$

Thus, the constant consists of paramagnetic and diamagnetic contributions. In the derivation of Eq. (8), the generalized Hellmann–Feynman theorem¹⁴ was used for elimination of second wave function derivatives. The first derivative of $|g\rangle$ may be obtained by standard coupled-perturbed calculations.⁶ Nevertheless, the paramagnetic perturbation terms [Eqs. (2)–(4)] cause a substantial increase of computer time and memory if compared to a single-point energy calculation. As indicated in the introduction, such a calculation of the wave function derivatives may be circumvented using the SOS expansions. A complete sum over all electronic states ($1 = \sum_j |j\rangle \langle j|$) can be inserted in Eq. (8) and the identity $[H, \partial/\partial I_{N\alpha}] = -\partial H/\partial I_{N\alpha}$ used, so that

$$J_{N\alpha M\beta}^P = - \sum_{j \neq g} \frac{2\hbar^2}{\epsilon_{jg}} \left\langle g \left| \frac{\partial H}{\partial I_{M\beta}} \right| j \right\rangle \left\langle j \left| \frac{\partial H}{\partial I_{N\alpha}} \right| g \right\rangle, \quad (9)$$

where $\epsilon_{jg} = \epsilon_j - \epsilon_g$ is the vertical electronic excitation energy. Although the Hamiltonian is a sum of more contributions, the terms (2)–(4) contribute to isotropic coupling separately.

The Hamiltonian for the spin–dipolar term [Eq. (3)] can be re-written using Cartesian components as

$$H_{SD} = \sum_{n,N,\alpha,\beta} s_{n\alpha} T_{\alpha\beta}^{nN} I_{N\beta}, \quad (10)$$

with $T_{\alpha\beta}^{nN} = (g_e g_N \mu_B \mu_N \mu_0) / (4\pi\hbar^2) (3r_{nN\alpha} r_{nN\beta} - \delta_{\alpha\beta} r_{nN}^2) / (r_{nN}^5)$. Sum (9) can be further simplified using properties of the spin operators and summing over all mono-excited triplet states ($|j\rangle = |K \rightarrow J\rangle$)

$$\begin{aligned} J_{NM}^{SD} &= - \frac{g_N g_M}{3} \left(\frac{g_e \mu_B \mu_N \mu_0}{4\pi} \right)^2 \sum_{\alpha=1}^3 \sum_{\beta=1}^3 \sum_{K, \text{occ}} \sum_{J, \text{virt}} \frac{1}{\epsilon_{jN}} \\ &\quad \times \langle K | \Theta_{N\alpha\beta} | J \rangle \langle J | \Theta_{M\alpha\beta} | K \rangle, \end{aligned} \quad (11)$$

where $\Theta_{N\alpha\beta} = (3r_{nN\alpha} r_{nN\beta} - \delta_{\alpha\beta} r_{nN}^2) / r_{nN}^5$ is a one-electron operator with $\mathbf{r}_N = \mathbf{r} - \mathbf{R}_N$. We reserve the letter K for occupied and J for virtual orbitals. Several approximations of excitation energies were used in the past.^{5,7–10} Most conveniently, the energies can be thought of as a difference of Kohn–Sham (KS) orbital energies

$$\epsilon_{jg} = \epsilon_J - \epsilon_K \quad (12a)$$

Latest studies indicate that such energies lie between singlet and triplet excitations for exact density functionals.¹⁵ Better results were obtained for polarizabilities⁷ with re-calculated HF molecular orbital (MO) energies (ϵ'_j, ϵ'_k) for KS orbitals used in a first-order approximation of singlet excitations

$$\epsilon_{jg} = \epsilon'_j - \epsilon'_k - J_{JK} + 2K_{JK}, \quad (12b)$$

where J_{JK} and K_{JK} is the usual coulomb and exchange integral, respectively. Analogously, for triplet excitation energies we get

$$\epsilon_{jg} = \epsilon'_j - \epsilon'_k - J_{JK} \quad (12c)$$

For the coupling, Eqs. (12a)–(12c) lead to similar results and thus the computationally least demanding Eq. (12a) was used in this study conveniently used for the bigger molecules.

Similarly as for SD, only triplet states contribute to the Fermi contact term. Because of the δ -function, only orbital amplitudes at the nuclei remain in final expression

$$\begin{aligned} J_{NM}^{FC} &= - \left(\frac{2\mu_0 g_e \mu_B \mu_N}{3} \right)^2 g_N g_M \\ &\quad \times \sum_K \sum_J \frac{\psi_J(r_N) \psi_K(r_N) \psi_J(r_M) \psi_K(r_M)}{\epsilon_{jN}} \end{aligned} \quad (13)$$

Note that although it is interesting to enumerate the FC and SD terms separately, it is easier to calculate their sum. Since

$$H_{FCSD} = H_{FC} + H_{SD} = \sum_{n,N} \sum_{\alpha} \sum_{\beta} s_{n\beta} t_{\beta\alpha} I_{N\alpha},$$

then the elements of $t_{\alpha\beta} = (\mu_0 g_e \mu_B \mu_N \gamma_N) / (4\pi\hbar) \times (\delta_{\alpha\beta} \sum_{\gamma} \partial^2 / (\partial R_{N\gamma} \partial R_{N\gamma}) (1/r_{nN}) - \partial^2 / (\partial R_{N\alpha} \partial R_{N\beta}) (1/r_{nN}))$ in atomic orbital basis can be calculated from derivatives of the Coulomb integral $\langle \chi_a | 1/r | \chi_b \rangle$.^{4,16}

Unlike FC and SD, the paramagnetic spin–orbit coupling depends only on singlet excitations. For the closed shell we get the working formula

$$\begin{aligned} J_{NM}^{PSO} &= - \frac{g_N g_M}{3} \left(\frac{e \mu_0 \mu_N}{2\pi m_e} \right)^2 \sum_K \sum_J \frac{1}{\epsilon_{jN}} \sum_{\alpha=1}^3 \left\langle K \left| \frac{l_{N\alpha}}{r_N^3} \right| J \right\rangle \\ &\quad \times \left\langle K \left| \frac{l_{M\alpha}}{r_M^3} \right| J \right\rangle. \end{aligned} \quad (14)$$

Finally, the diamagnetic part, similarly as in Ref. 4, was calculated using a numerical integration of electron density, ρ

TABLE I. Calculated and observed coupling constants [Hz] in small molecules.

Compound	Coupling constant	SOS ^a	CP/HF ^b	CP/DFT ^c	Exp. ^d
CH ₄	¹ J(C, H)	62.0	143	122.3	124.0
	² J(H, H)	-1.9	-24	-6.4	-12.4
CH ₃ -CH ₃	¹ J(C, C)	20.2	52.7	30.2	34.6
	¹ J(C, H)	61.4	143.1	123.8	125.0
	² J(C, H)	2.6	-11.3	-1.8	-4.8
	³ J(H, H) <i>trans</i>	6.0	17.6	14.5	8.0 (averaged)
CH ₂ =CH ₂	³ J(H, H) <i>gauche</i>	0.8	5.1	2.6	
	¹ J(C, C)	45.2	642	68.6	67.6
	¹ J(C, H)	71.7	443	145.3	156.4
	² J(C, H)	4.6	-279	1.8	-2.4
	² J(H, H)	2.5	-176	3.7	2.5
	³ J(H, H) <i>cis</i>	3.6	182	6.5	11.6
CH≡CH	³ J(H, H) <i>trans</i>	5.4	207	12.1	19.1
	¹ J(C, C)	165.9	416	204.9	170.6
	¹ J(C, H)	90.8	389	238.9	248.7
	² J(C, H)	23.0	-52	47.4	49.7
	³ J(H, H)	3.4	81	2.5	9.8
H ₂ O	² J(H, H)	-2.6	-23.9	-10.8	-7.2
	¹ J(O, H)	-162.3	-91.9	-402.3	-390.9
CH ₃ F	¹ J(C, H)	68.9	172.4	142.3	149.2
	² J(H, H)	0.1	-21.0	-2.76	-9.6
	² J(F, H)	27.0	55.4	33.2	46.5
	¹ J(C, F)	-221.9	-122.6	-262.2	-162.0
N ₂	¹ J(N, N)	-3.8	14.2	-0.037	-2.47
H ₂	¹ J(H, H)	183.2	300.4	338.7	279.9
HF	¹ J(H, F)	129.3	576.4	388.9	530.2

^aB3LYP/6-31G** calculation, Eqs. (12b) and (12c).

^b6-311++G** basis.

^cReference 6, local spin-density approximation with a combined double/triple-zeta doubly polarized STO basis.

^dExperimental values for light hydrocarbons from Ref. 23, otherwise Ref. 6.

$$J_{NM}^{\text{DSO}} = \frac{g_N g_M e^2 \mu_0^2 \mu_N^2}{24 \pi^2 m_e} \int \rho(\mathbf{r}) \frac{\mathbf{r}_N \cdot \mathbf{r}_M}{r_M^3 r_N^3} d\mathbf{r}. \quad (15)$$

For the integration a variable Cartesian grid was used and a numerical error of about 10% was considered acceptable because of the small relative magnitude of this contribution. An alternate option would require an estimation of AO integrals $\langle \chi_a | r_{N\beta} r_{M\beta} r_N^{-3} r_M^{-3} | \chi_b \rangle$, which can be done using a numerical integration¹⁷ or expansions of the integrated functions.¹⁸

III. COMPUTATIONS

Molecular geometries were optimized with the GAUSSIAN set of programs.¹ The Becke3LYP (B3LYP) hybrid HF-DFT functional¹⁹ was used for the optimization and SOS calculation with basis sets described in Sec. V. Then the energies and orbital coefficients were read by the Roa programs, where the SOS formulas were implemented. For the comparative coupled-HF calculations of coupling constants, the DALTON program package² was used. Computations were performed at graphic workstations (185–190 MHz CPU clock) at the Institute of Organic Chemistry and Biochemistry and at the Supercomputer Center of Charles University.

IV. EXPERIMENT

Proton and carbon-13 NMR spectra of α -pinene, β -pinene, and camphor were measured on Fourier-transform-nuclear magnetic resonance (FT-NMR) spectrometer Varian UNITY-500 (¹H at 500 MHz; ¹³C at 125.7 MHz) Proton-

proton coupling constants were obtained by the first-order analysis from expanded spectra. Lorentz–Gauss weighting function was used for the resolution enhancement.

V. RESULTS AND DISCUSSION

A. Small molecules

Nuclear spin–spin coupling constants in nine small molecules were calculated using the SOS scheme and the coupled-HF (CP/HF) method. In Table I, these results are compared to the experimental values and a former CP/DFT calculation from Ref. 6. For all molecules B3LYP/6-31G** optimized geometries were used. As can be seen in the table, the SOS values are in the average underestimated by about 50%, while the CP/HF calculation tends to overestimate the coupling by about 100%–1000%. The most advanced CP/DFT calculation [with the valence triple zeta (VTZ) (Slater-type orbitals (STO)) basis] best reproduces the experimental results. The overall error of the SOS results is smaller than that of the CP/HF calculation. Since the SOS method also reasonably reproduces relative differences between molecules and kinds of coupling constants, it can be considered as a reasonable compromise with respect to accuracy and computing cost.

The error of calculated results depends on the kind of interaction. For ³J(H, H) values accuracy of the SOS and CP/DFT methods is comparable. For ethylene, the SOS constants (3.5 and 5.4 Hz for the *cis*- and *trans*-arrangement, respectively) are farther from the experiment (11.6 and 19.1

TABLE II. The dependence of coupling constants in C_2H_4 on the basis set size. Equations (12b) and (12c) are used.

Coupling constant	Basis	631G	631G**	631+ + G**	AUG	Exp. (Ref. 22)
		26 b.f.	50 b.f.	62 b.f.	210 b.f.	
$^1J(C, C)$	FC	47.4	50.2	44.5	49.1	67.6
	PSO	-7.3	-7.2	-6.9	-8.0	
	SD	2.3	2.2	1.6	1.8	
	DSO	0.1	0.0	0.1	0.0	
	total	42.4	45.1	39.1	43.0	
$^1J(C, H)$	FC	84.3	70.6	75.0	80.1	156.4
	PSO	0.3	0.3	0.3	0.5	
	SD	0.2	0.2	0.2	0.2	
	DSO	0.6	0.6	0.6	1.0	
	total	85.4	71.7	76.1	82.0	
$^2J(C, H)$	FC	5.5	6.1	6.2	5.1	-2.4
	PSO	-1.2	-1.0	-0.9	-0.8	
	SD	0.1	0.1	0.1	0.1	
	DSO	-0.6	-0.7	-0.7	-0.7	
	total	3.7	4.6	4.7	3.7	
$^2J(H, H)$	FC	3.7	3.6	4.4	4.2	2.5
	PSO	1.3	2.5	2.5	3.4	
	SD	0.2	0.1	0.1	0.2	
	DSO	-3.5	-3.7	-3.7	-3.8	
	total	1.8	2.5	3.2	4.0	
$^3J(H, H)_{cis}$	FC	5.4	4.3	3.7	-0.4	11.6
	PSO	-0.1	0.4	0.4	0.7	
	SD	0.0	0.0	0.0	0.0	
	DSO	-1.0	-1.0	-1.0	-1.0	
	total	4.3	3.6	3.0	-0.7	
$^3J(H, H)_{trans}$	FC	8.1	7.3	7.4	7.0	19.1
	PSO	0.1	1.5	1.6	2.5	
	SD	0.5	0.1	0.1	0.1	
	DSO	-3.4	-3.5	-3.5	-3.5	
	total	5.3	5.4	5.6	6.0	

Hz) than the CP/DFT results (6.5 and 12.1 Hz), while for acetylene the SOS value of the constant $^3J(H, H) = 3.4$ is more realistic than for the CP calculation, although still substantially underestimated. Generally, a poor performance of all calculations can be observed for $^2J(H, H)$ and $^2J(C, H)$ constants where namely the negative experimental values (see CH_4 , C_2H_6 , H_2O , and CH_3F) are not well reproduced.

Dependence of the SOS results on the size of basis set can be seen in Table II for ethylene. Rather ambiguous conclusions can be made. On one side, the results are apparently quite numerically stable and almost independent on the basis. This would enable *ab initio* calculation of the couplings in “giant” molecules unavailable for other computational techniques. On the other side, this stability prevents further improvement of the method and shows the limit of the rigid-orbital model and other approximations that had to be

TABLE IV. The dependence of the CPU time on the size of the basis set, for C_2H_4 .

Basis	DFT(SOS)		CHF(SCF)	
	t [s]	$^1J(C, C)$	t [s]	$^1J(C, C)$
6-31G	52	54	41	-467
6-31G**	67	55	101	-1062
6-31+ + G**	89	48	249	1318
6-311+ + G**	103	40	273	600
cc-pVTZ	313	67	1180	560

currently anticipated. As may be expected, the paramagnetic terms are more sensitive to the size of the basis than the diamagnetic part.

Four different models for the excited electronic states and energies were considered for the C_2H_4 molecule. The results summarized in Table III. The DFT calculations with [Eqs. (12b) and (12c)] or without [Eq. (12a)] the singlet-triplet corrections yield better values for the coupling than the HF model. Especially the rigid-orbital HF approximation (second column in the table) leads to poor results namely for the longer-range $^3J(H, H)$ constants. This can be expected since lower-energy “volatile” orbitals [e.g., highest occupied molecular orbital (HOMO) and lowest unoccupied molecular orbital (LUMO), most affected by the spin corrections in Eqs. (12b) and (12c)] participate more on the remote coupling.

The CP/HF calculation not only yields worse results than SOS, but is also more demanding on computer resources. This is documented in Table IV, where computer time for the SOS and CPHF [self-consistent field (SCF)] calculations are compared. Evidently, the SOS method scales better with the number of basis functions and is numerically more stable. The CPHF calculation even gives opposite sign of the $^1J(C, C)$ constant for smaller bases. However, the time of calculation strongly depends on actual computer implementation. For the calculation shown in Table IV, Eq. (12a) was used for the SOS method, while calculations of energies according to Eqs. (12b) and (12c) required longer times. Also the numerical integration [Eq. (15)] becomes more time consuming when a finer grid is used.

B. Terpenes

To test the performance of the method for bigger systems we have chosen β -pinene, α -pinene and camphor, see Fig. 1 for the structure and atomic numbering. These mol-

TABLE III. The dependence of the SOS coupling constants in C_2H_4 on the excitation energies.

Model:	HF	HF	DFT	DFT	Exp. (Ref. 22)
	[Eq. (12a)]	[Eqs. (12b) and (12c)]	[Eq. (12a)]	[Eqs. (12b) and (12c)]	
$^1J(C, C)$	38.7	41.7	45.1	55.0	67.6
$^1J(C, H)$	49.2	63.0	71.7	78.6	156.4
$^2J(C, H)$	3.5	4.4	4.6	5.1	-2.4
$^2J(H, H)$	0.8	1.7	2.5	4.1	2.5
$^3J(H, H)_{cis}$	0.72	2.1	3.6	3.3	11.6
$^3J(H, H)_{trans}$	0.6	4.4	5.4	5.0	19.1

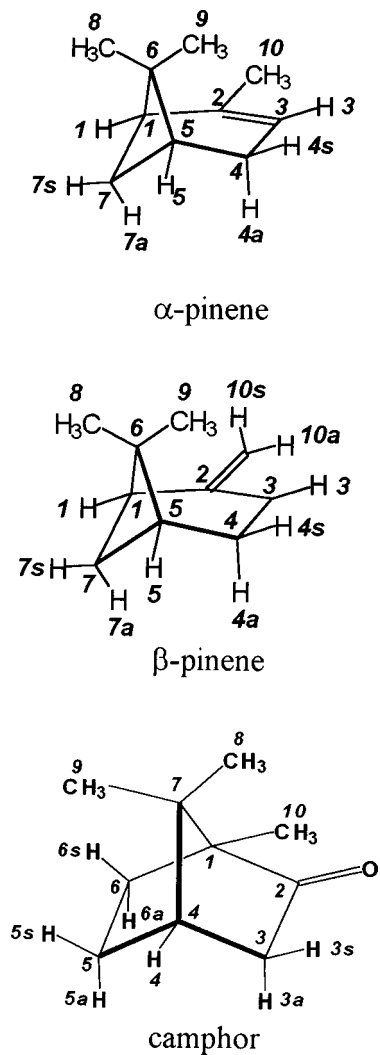


FIG. 1. α -Pinene, β -pinene, and camphor—numbering of carbon and hydrogen atoms.

ecules are relatively nonpolar and rigid, in favor of the *ab initio* modeling targeting molecules in vacuum. Their VCD and ROA spectra, also dependent on the magnetic properties of the electron clouds, were found to be almost independent on the solvent.^{20,21} Thus, we suppose that NMR spectra are not too sensitive to solvent effects as well. This is also indicated by the data for coupling constants in β -pinene, listed in Table V for four different solvents, CCl_4 , C_6D_6 , CDCl_3 and CD_3COCD_3 . Apparently, the inclusion of the extra term in Eqs. (12b) and (12c) (third column in the table) does not lead to any improvement in this case. Similarly as for the small hydrocarbons, the calculated shorter-range ${}^2J(\text{H},\text{H})$ constants are predicted with largest error. On the contrary, the longer-range constants approximately match in their relative magnitudes found experimentally. This can be seen on the correlation diagram in Fig. 2 where a complete set of calculated constants is compared to experiment from Ref. 23. The $-\text{CH}_3$ group is not included because of many theoretical (a relevant theory for the semi-free rotor has not been yet developed) and experimental (small splitting with limited information about geometry) obstacles. Typically, calculated constants are 2 to 3 times smaller than experimental values. This is true also for α -pinene and more polar camphor, for which the coupling constants are listed in Tables VI and VII, respectively. Thus we can conclude that the method gives approximate relative magnitudes of longer-range hydrogen coupling constants (${}^nJ(\text{H},\text{H})$, $n > 2$), while the absolute magnitudes are significantly underestimated. Unfortunately, combined errors of the FC, PSO, SD, and DSO contributions do not enable reliable calculations of constants smaller than about 0.5 Hz.

While the FC and SD contributions to the coupling stem from the spin magnetic moment of electrons, the PSO and DSO terms arise from electronic charge (producing orbital

TABLE V. Calculated and experimental coupling constants ${}^nJ(\text{H}_i, \text{H}_j)$ for β -pinene.

n	H_i, H_j	Calc.		Exp.			
		Eq. (12a)	Eqs. (12b) and (12c)	CD_3COCD_3 (Ref. 23)	C_6D_6 (Ref.23)	CCl_4 (Ref. 24)	CDCl_3
2	3a,3s	-1.74	-1.85	-17.44	-17.41	-18.0	-17.5
	4s,4a	-0.65	-0.75	-13.30	-13.32	-13.5	-13.3
	7s,7a	0.24	-0.20	-9.83	-9.84	-10.0	-9.8
	10a,10s	3.85	2.10	2.09	1.99	1.5	2.2
3	1, 7s	2.26	1.83	5.56	5.57	5.5	5.8
	3a,4s	2.32	1.59	7.67	7.63	7.4	7.8
	3a,4a	4.07	3.29	10.79	10.76	9.7	10.2
	3s,4s	3.46	2.80	9.27	9.30	8.5	8.4
	3s,4a	-0.37	-0.55	1.61	1.65	2.5	2.4
	4a, 5	1.9	1.66	4.44	4.42	4.0	4.2
	4s, 5	0.31	0.21	1.80	1.82	2.0	2.1
	5, 7a	-0.42	-0.43	0.52	0.53	a	<0.5
4	5, 7s	2.33	1.94	6.07	6.06	5.8	6.1
	1, 5	1.32	0.78	5.32	5.32	5.0	5.4
	1, 10s	0.75	0.83	-0.54	-0.55	a	-0.5
	3a,10a	-0.08	0.00	-2.53	-2.51	-2.5	-2.4
	3a,10s	-0.59	-0.63	-2.96	-2.93	-2.5	-2.9
	3s,10a	0.61	0.78	-1.26	-1.27	-1.3	-1.2
	3s,10s	-0.41	-0.57	-1.15	-1.17	-1.3	-1.2
5	4s,7s	0.15	-0.13	1.53	1.55	1.5	1.2
	10s,4a	-0.23	-0.45	0.51	0.5		
	3a,7s	-0.1	-0.43	0.51	~0.5		

^aNot given.

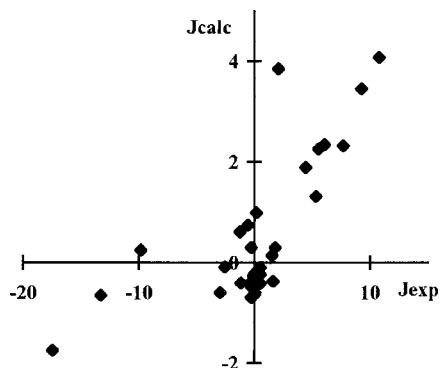


FIG. 2. Calculated vs experimental coupling constant [$J(\text{H}, \text{H})$] for β -pinene.

magnetic moment). Although the magnitudes of these two moments are similar, their interaction with the electron density is different. In Fig. 3, we have plotted the dependence of these two coupling contributions on the distance of the hydrogen atoms in β -pinene. Clearly, the spin contribution (FC+SD) is much bigger than the orbital part for smaller distances. However, the orbital part (PSO+DSO) appears not to fade so quickly with the distance and its relative contribution is thus supposedly bigger for longer-range interactions. This reflects the locality of the spin while the orbital moment is more spread over the space. Obviously, magnitude of individual coupling constants strongly varies according to the chemical structure.

The relatively big error of calculated coupling constants is in a contrast with the accuracy that can be achieved for the magnetic shielding (chemical shift). This can be compared in Table VIII, where isotropic shielding tensors for carbon and hydrogen atoms are listed for the three terpenes, as calculated by Gaussian at the Becke3LYP/6-31G** level. Rather surprisingly, the influence of the solvent is also small (cf. CHCl_3 and C_6H_6 for β -pinene) and calculated chemical shifts agree with observed values within few %. As the NMR signal of several atoms was miss-assigned in the past ($\text{H}_{3a,3b}; \text{H}_{10a,10b}; \text{Me}_8, \text{Me}_9$)²³ present computational tools apparently enable unambiguous assignment.

TABLE VI. Calculated and experimental coupling constants ${}^nJ(\text{H}_i, \text{H}_j)$ in α -pinene. Equation (12a) used.

n	H_i, H_j	Calc.	CDCl_3
2	4a,4s	-1.9	-17.3
	7a,7s	0.8	-8.5
3	1, 7s	2.3	5.5
	3, 4a	0.7	3.0
	3, 4s	0.6	2.8
	4a, 5	1.1	2.8
	4s, 5	0.9	2.8
4	5, 7s	2.3	5.7
	1, 3	0.1	1.6
	1, 5	1.5	5.7
	3, 5	0.0	1.6

TABLE VII. Calculated and experimental coupling constants ${}^nJ(\text{H}_i, \text{H}_j)$ in camphor. Equation (12a) used.

n	H_i, H_j	Calc.	CDCl_3
2	3a,3s	-2.2	-18.2
	5a,5s	-0.4	-12.1
	6a,6s	-0.7	-13.6
3	3a, 4	-0.2	~ 0
	3s, 4	1.9	4.6
	4, 5a	-0.2	~ 0
	4, 5s	1.7	4.5
	5a,6a	3.7	9.5
	5a,6s	0.6	3.6
	5s,6a	0.8	4.5
	5s,6s	4.4	11.6
4	3s,5a	0.1	0.3
	3s,5s	-0.6	3.1
	4, 6s	-0.24	0.8

C. The role of electronic density

The integrated function in Eq. (15) can be interpreted as a diamagnetic coupling density $D(r)$

$$J_{NM}^{\text{DSO}} = \int D(r) dr. \quad (16)$$

Although the diamagnetic part plays a rather minor role, its graphical representation may become a useful tool, allowing one to estimate the relation between the coupling and chemical structure. Note, that also the paramagnetic parts of the coupling Hamiltonian have singularities in the nuclei with a rational decay ($\sim r^{-n}$), similarly as for $D(r)$. Typically, sign of J^{DSO} is negative (cf. the values in Table II), since $\mathbf{r}_N \cdot \mathbf{r}_M \sim D(\mathbf{r}) < 0$ between atoms connected by set of covalent bonds. Positive DSO coupling can arise only with a substantial contribution from regions outside the space between the coupled pair, e.g., for ${}^2J(\text{C}, \text{H})$ in C_2H_4 where most of the electrons are concentrated around the double bond $\text{C}=\text{C}$.

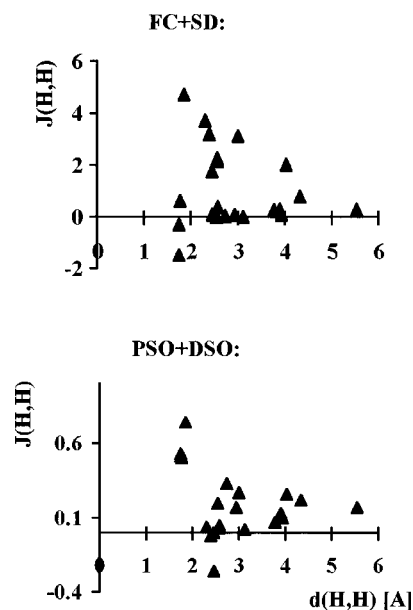


FIG. 3. The dependence of (FC+SD) and (PSO+DSO) coupling contributions on atomic distance in β -pinene.

TABLE VIII. Calculated isotropic shielding constants and the observed chemical shifts of carbons and protons in β -pinene, α -pinene and camphor.^a

β -pinene				α -pinene			camphor		
Atom	Calc.	CDCl ₃	C ₆ D ₆ (Ref. 21)	Atom	Calc.	CDCl ₃	Atom	Calc.	CDCl ₃
C-1	53.0	52.1	51.8	C-1	60.9	57.66	C-1	48.2	47.3
C-2	147.2	151.3	152.3	C-2	209.4	219.62	C-2	142.8	144.1
C-3	26.8	23.8	23.6	C-3	43.8	43.26	C-3	115.5	116.2
C-4	26.3	23.6	23.6	C-4	46.1	43.02	C-4	33.4	31.5
C-5	42.5	40.8	40.4	C-5	29.8	27.02	C-5	42.8	41.5
C-6	45.8	40.8	40.6	C-6	32.2	29.88	C-6	43.2	38.0
C-7	28.1	27.0	27.0	C-7	50.8	46.75	C-7	34.2	31.4
C-8	26.1	25.8	26.1	C-8	21.0	19.11	C-8	26.4	28.8
C-9	22.4	21.7	21.8	C-9	20.5	19.74	C-9	21.0	26.5
C-10	104.1	106.3	105.9	C-10	12.5	9.21	C-10	23.6	20.8
H-1	2.55	2.45	2.51	H-1	2.08	1.93	H-3a	1.71	1.85
H-3a	2.60	2.54	2.52	H-3	5.49	5.18	H-3s	2.32	2.35
H-3s	2.14	2.25	2.21	H-4a	2.29	2.23	H-4	2.01	2.09
H-4a	1.74	1.82	1.81	H-4s	2.35	2.15	H-5a	1.30	1.34
H-4s	1.97	1.85	1.86	H-5	2.10	2.07	H-5s	2.04	1.95
H-5	2.05	1.97	1.91	H-7a	1.27	1.15	H-6a	1.42	1.41
H-7a	1.55	1.42	1.42	H-7s	2.38	2.33	H-6s	1.79	1.68
H-7s	2.25	2.32	2.28	Me-8	1.22	1.26	Me-8	0.87	0.84
Me-8	1.20	1.24	^b	Me-9	0.98	0.84	Me-9	1.00	0.96
Me-9	0.85	0.72	^b	Me-10	1.65	1.66	Me-10	0.95	0.92
H-10a	4.82	4.62	4.77						
H-10s	4.81	4.56	4.73						

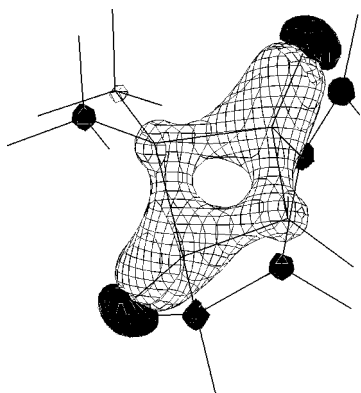
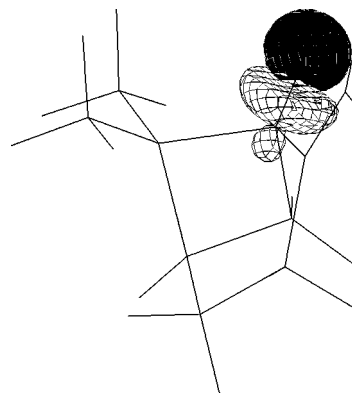
^aB3LYP/6-31G**, average values for the three methyl group hydrogen atoms are given.^bNot given.

As a typical example, $D(\mathbf{r})$ for the $^4J(\text{H}_1, \text{H}_5)$ coupling constant in β -pinene is plotted in Fig. 4. The negative coupling is enhanced by the four-member cycle, which can also explain the unusually high (although positive) magnitude of the total coupling constant. The remaining cycle contributes positively and, surprisingly, contributions of the methyl groups do not have same signs.

The paramagnetic part of the coupling is more complex. Nevertheless, the influence of a particular atomic magnetic moment on electronic density can be visualized. For the Fermi contact term, a change of spin-polarized electronic density caused by an atom N is equal to

$$\frac{\partial \rho_\alpha(\mathbf{r})}{\partial \mu_{Nz}} = 2 \sum_{K\alpha} \sum_{J\alpha} \psi_K(\mathbf{r}) \frac{\langle K | \partial H / \partial \mu_{Nz} | J \rangle}{\epsilon_{jn}} \psi_J(\mathbf{r}) \\ \sim \sum_K \sum_J \epsilon_{jn}^{-1} \psi_K(\mathbf{r}) \psi_K(r_N) \psi_J(\mathbf{r}_N) \psi_J(\mathbf{r}). \quad (17)$$

In Fig. 5, regions with the largest amplitude of this function are plotted for H₁ of β -pinene. Apparently, the disturbance of the electronic density caused by the FC interaction is quite localized and aligned along the C–H bond. Similarly, we can define an analogous “derivative” of electronic density for the PSO contribution

FIG. 4. β -Pinene, isodensity surface for the diamagnetic coupling between H₁ and H₅.FIG. 5. β -Pinene, spin-polarized electronic density perturbed by the FC interaction with H₁.

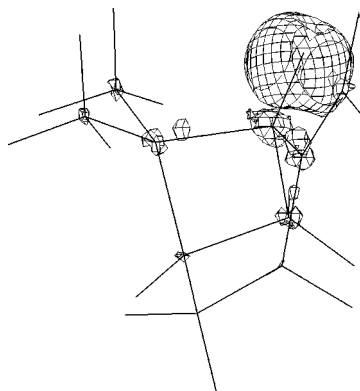


FIG. 6. β -Pinene, change of electronic density caused by the PSO interaction with H_1 .

$$\frac{\partial \rho(\mathbf{r})}{\partial \mu} = \sqrt{\left(\frac{\partial \rho(\mathbf{r})}{\partial \mu_x}\right)^2 + \left(\frac{\partial \rho(\mathbf{r})}{\partial \mu_y}\right)^2 + \left(\frac{\partial \rho(\mathbf{r})}{\partial \mu_z}\right)^2}. \quad (18)$$

This function is plotted in Fig. 6, approximately with the same isodensity limit as in Fig. 5. Unlike FC, the PSO disturbance is significantly less localized. Thus it may be expected that the PSO part is more susceptible to changes of chemical structure and solvent.

The paramagnetic parts (FC+SD+PSO) also determine the influence of chemical environment on the coupling, in contrast to the diamagnetic part mostly given by the geometry of nearest bonds. For example, diamagnetic parts of the constants $J(H_{7a}, H_{7s})$ and $J(H_{4a}, H_{4s})$ are similar (-1.77 and -1.66 Hz, respectively) while the paramagnetic FC terms have opposite signs (0.46 and -0.55 Hz).

VI. CONCLUSIONS

The sum-over-states calculation of the nuclear spin–spin coupling constants is faster than the coupled-perturbed techniques while the accuracy of the results is comparable for bigger systems. Relative magnitudes of most H–H coupling constants in β -pinene, α -pinene, and camphor were correctly predicted by the calculation, while their absolute magnitudes were typically 2 to 3 smaller than found by the experiment.

ACKNOWLEDGMENT

The work was supported by the Grant Agency of the Czech Republic (Grant No. 203/97/P002).

- ¹GAUSSIAN 94, Revision E.2, M. J. Frisch, G. W. Trucks, H. B. Schlegel, P. M. W. Gill, B. G. Johnson, M. A. Robb, J. R. Cheeseman, T. Keith, G. A. Petersson, J. A. Montgomery, K. Raghavachari, M. A. AllLaham, V. G. Zakrzewski, J. V. Ortiz, J. B. Foresman, J. Cioslowski, B. B. Stefanov, A. Nanayakkara, M. Challacombe, C. Y. Peng, P. Y. Ayala, W. Chen, M. W. Wong, J. L. Andres, E. S. Replogle, R. Gomperts, R. L. Martin, D. J. Fox, J. S. Binkley, D. J. Defrees, J. Baker, J. P. Stewart, M. Head-Gordon, C. Gonzalez, J. A. Pople, Gaussian, Inc., Pittsburgh, PA, 1995; for a coupled-perturbed calculation of spin coupling with a modified version of GAUSSIAN see, T. Bandyopadhyay, J. Wu, W. A. Stripe, I. Carmichael, and A. S. Serianni, *J. Am. Chem. Soc.* **119**, 1737 (1997).
- ²DALTON, Release 1.0, T. Helgaker, H. J. Aa. Jensen, P. Jørgensen, J. Olsen, K. Ruud, H. Ågren, T. Andersen, K. L. Bak, V. Bakken, O. Christiansen, P. Dahle, E. K. Dalskov, T. Enevoldsen, B. Fernandez, H. Heiberg, H. Hettema, D. Jonsson, S. Kirpekar, R. Kobayashi, H. Koch, K. V. Mikkelsen, P. Norman, M. J. Packer, T. Saue, P. R. Taylor, and O. Vahtras (1997).
- ³J. R. Cheeseman, G. W. Trucks, T. A. Keith, and M. J. Frisch, *J. Chem. Phys.* **104**, 5497 (1996).
- ⁴O. Vahtras, H. Ågren, P. Jørgensen, H. J. Aa. Jensen, S. B. Padkjær, and T. Helgaker, *J. Chem. Phys.* **96**, 6120 (1992).
- ⁵V. G. Malkin, O. Malkina, L. A. Eriksson, R. D. Salahub, in *Modern Density Functional Theory*, edited by J. M. Seminario and P. Politzer (Elsevier, Amsterdam, 1995).
- ⁶G. Schreckenbach, R. M. Dickson, Y. R. Morales and T. Ziegler, in *Chemical Applications of Density-Functional Theory*, edited by B. B. Laird, R. B. Ross, and T. Ziegler (American Chemical Society, Washington, DC 1996), Chap. 23.
- ⁷P. Bouř, *Chem. Phys. Lett.* **265**, 65 (1997).
- ⁸P. Bouř, J. McCann, and H. Wieser, *J. Chem. Phys.* **108**, 8782 (1998).
- ⁹P. Bouř, J. McCann, and Hal Wieser, *J. Phys. Chem. A* **101**, 9783 (1997).
- ¹⁰P. Bouř, *Chem. Phys. Lett.* **288**, 363 (1998).
- ¹¹H. Fukui and T. Baba, *J. Chem. Phys.* **108**, 3854 (1998).
- ¹²N. F. Ramsey, *Phys. Rev.* **91**, 303 (1953).
- ¹³P. O. Åstrand, K. V. Mikkelsen, P. Jørgensen, K. Ruud, and T. Helgaker, *J. Chem. Phys.* **108**, 2528 (1998).
- ¹⁴R. G. Parr and W. Yang, *Density-functional Theory of Atoms and Molecules* (Oxford University Press, New York, 1989).
- ¹⁵C. Filippi, C. J. Umrigar, and X. Gonze, *J. Chem. Phys.* **107**, 9994 (1997).
- ¹⁶P. M. W. Gill, in *Advances in Quantum Chemistry*, edited by P. O. Löwdin (Academic, San Diego, 1994), Vol. 25, p. 143.
- ¹⁷O. Matsuoka and T. Aoyama, *J. Chem. Phys.* **73**, 5718 (1980).
- ¹⁸An expansion of $(1/r)$ into Gaussian s -functions was also implemented in the Roa program. Then the identity $r_{Na}r_{M\beta}/r_N^3r_M^3 = [\partial(1/r_N)/\partial r_{N\alpha}] \times [\partial(1/r_M)/\partial r_{M\beta}]$ allows one to expand also the diamagnetic integrals. The method, however, was not numerically stable and the direct integration was preferred.
- ¹⁹A. D. Becke, *J. Chem. Phys.* **98**, 5648 (1993).
- ²⁰P. Bouř, J. McCann, and H. Wieser, *J. Phys. Chem. A* **102**, 102 (1998).
- ²¹P. Bouř, V. Baumruk, and J. Hanzlíková, *Collect. Czech. Chem. Commun.* **9**, 1384 (1997).
- ²²D. M. Graham and C. E. Holloway, *Can. J. Chem.* **41**, 2114 (1963).
- ²³E. Kolehmainen, K. Laihia, R. Laatikainen, J. Vepsäläinen, M. Niemitz, and R. Suontamo, *Magn. Reson. Chem.* **35**, 463 (1997).
- ²⁴R. J. Abraham, M. A. Cooper, H. Indyk, T. M. Siverns, and D. Whittaker, *Org. Magn. Reson.* **5**, 373 (1972).